



A Facile Phyto-Mediated Synthesis of Gold Nanoparticles using Aqueous Extract of *Momordica cochinchinensis* Rhizome and Their Biological Activities

A. Lakshmanan, C. Umamaheswari, N.S. Nagarajan*

Department of Chemistry, Gandhigram Rural Institute - Deemed University, Gandhigram - 624 302, Tamil Nadu, India

ARTICLE DETAILS

Article history:

Received 03 January 2016

Accepted 12 January 2016

Available online 26 February 2016

Keywords:

Gold Nanoparticles

Momordica cochinchinensis

Antioxidant

Antibacterial Activity

ABSTRACT

In the present study, plant mediated synthesis of gold nanoparticles (AuNPs) using aqueous extract of *Momordica cochinchinensis* rhizome at room temperature as a reducing as well as a stabilizing agent is reported. The gold nanoparticles synthesized by a green chemical approach were characterized by UV-visible spectroscopy; Transmission Electron Microscopy (TEM), Energy Dispersive X-ray (EDX), X-ray Diffraction (XRD) and Fourier transform infrared (FT-IR) spectroscopy. The formation of AuNPs, observed by colour changes from yellow to ruby red is confirmed by UV-visible spectroscopy showing surface plasma resonance band that at 535 nm. The crystalline nature of the AuNPs formed as face centered cubic structure is evident from the selected area electron diffraction (SAED) and XRD pattern. FT-IR spectrum showed the presence of different biomolecules in the *Momordica cochinchinensis* rhizomes aqueous extract responsible for the reduction and stabilization of AuNPs. Phytosynthesized AuNPs showed better antioxidant activity than the aqueous extract when analysed by using DPPH, NO, H₂O₂ and reducing power assay methods. Moreover, the biosynthesized AuNPs significantly inhibited the growth of medically important pathogenic gram positive bacteria and gram negative bacteria.

1. Introduction

Recently, noble metal nanoparticles such as Au, Ag, Pt, and Pd are widely developed due to their special physio chemical properties in biological applications. Among several noble metal nanoparticles, gold nanoparticles (AuNPs) possess special optical and electronic properties [1]. The synthesis of gold nanoparticles (AuNPs) has gained significance as they possess unique chemical, physical, biological and optoelectronic properties which depend on the shape and size of nanoparticles and are exploited in a wide range of applications in biology, chemical sensing of single molecule, controlled release, catalysis, and immunoassays [2].

Gold nanoparticles (AuNPs) in the size range of 1–100 nm exhibit unique optical, electronic and catalytic properties compared to the bulk solids and they are biocompatible and non-toxic [3]. The synthesis of nanoparticles may involve two methods such as top down and bottom up approaches. Top down techniques, involve that decrease the size of the mass materials in the scope of nanoscale and in a bottom up technique the beginning materials are developed to bigger structures (nano) by joining atoms [4]. Several techniques are available for the synthesis of mono dispersed metal nanoparticles through physical and chemical methods [5].

Plant mediated synthesis of AuNPs is gaining more importance over other environmentally benign processes because the synthetic methods involve various chemicals that may lead to the presence of toxic chemical species adsorbed on the surface, which may have adverse effects in biological applications [6]. Currently a lot of research studies leading to novel methods of green synthesis of AuNPs have been carried as these methods are cost effective, free of hazardous reagents and involve only mild reaction conditions [7, 8] and these techniques involved mostly the use of enzymes and microorganisms like bacterium, fungi and yeast. Nanoparticles of various shapes have been synthesized by using microorganisms [9] and marine algae [10] and some of the major disadvantages in such methods are mistreatment of microbes, the need of manipulation of reaction parameters like pH, temperature and incubation time for the synthesis of nanoparticles [11]. Many researchers have synthesized gold nanoparticles using plants [12], extracts of *Syzygium*

aromaticum [13], *Curcuma pseudomontanav* [14], *Aloe vera* [15], *Camellia sinensis* [16] and *Psidium guajava* [17].

Most of the oxidative diseases are due to free radicals resulting in oxidative stress [18]. Free radicals such as superoxide anion, hydroxyl radicals and non-radical species such as hydrogen peroxide, singlet oxygen are different forms of activated oxygen constituting reactive oxygen species (ROS). Active anti-oxidative defense system is required to balance the production of free radicals. The oxidative damage induced by free radical generation is a critical etiological factor concerned with several chronic human diseases such as diabetes, cancer, mellitus, arthritis and neurodegenerative diseases and also in the aging process [19] and it is in the treatment of these diseases, anti-oxidant therapy has gained an enormous importance. The AuNPs and AgNPs are reported for diverse biological applications. Recently, reports of the antioxidant potential of Au and Ag nanoparticles have been published [20] and AuNPs have been used recently as free radical scavengers both in *in-vitro* and *in-vivo* models [21].

The gold nanoparticles possess higher antibacterial efficacy because of their larger total surface area per unit volume [22]. AuNPs exhibit excellent bactericidal activity on a range of microorganisms; its bactericidal effect depends on the size and the shape of the particles. It is well known that silver and gold nanoparticles can act as antibacterial and antifungal agents, due to their ability to interact with microorganisms [23].

Momordica cochinchinensis (family: Cucurbitaceae) is a tropical plant grown in many countries in tropical regions. It is called by different names such as gac (in Viet Nam), Bhat Kerala (in India) and Moc Niet Tu (in China) [24]. In East and Southeast Asia, it is used as a food and as traditional medicine. As a medicinal plant, in Viet Nam, the seed membranes are used to aid in the relief of dry eyes. Similarly, in traditional Chinese medicine the seeds of gac, known as mubiezi, are employed for a variety of internal and external purposes. This plant has been identified to as a valuable and effective source of natural antioxidants like phenolic acids, flavonoids, lycopene, β -carotene, α -tocopherol and lutein [24].

Herein, in the present study we report a very mild and environmentally benign phytomediated method for the synthesis of AuNPs using aqueous extract of *M. cochinchinensis* rhizome without any capping or stabilizing agent. The AuNPs synthesized were characterized by Ultra Violet Visible spectroscopy, Fourier transform-infrared spectroscopy, Energy Dispersive X-ray (EDX), High Resolution Transmission Electron Microscopy (HR-TEM), and X-ray diffraction studies. The synthesized MCR-AuNPs when tested for their antioxidant activity by *in vitro* methods

*Corresponding Author

Email Address: nsnrajan@yahoo.co.in (N.S. Nagarajan)

showed better antioxidant activity than the aqueous extract and moderate antibacterial activity when tested by disk diffusion method against tested gram positive and gram negative pathogens.

2. Experimental Methods

2.1 Chemicals

All chemicals of analytical grade were obtained commercially and were used without further purification. $\text{HAuCl}_4 \cdot 3\text{H}_2\text{O}$ (99.9%), 1,1-diphenyl-2-picryl-hydrazyl (DPPH), phosphate buffer and ascorbic acid were purchased from Sigma-Aldrich, Mumbai, India. All the aqueous solutions were prepared using Milli Q water.

2.2 Preparation of MCR Aqueous Extracts

Fresh and healthy rhizomes of *M. cochinchinensis* were washed several times with de-ionized water to remove the dust materials. Ten grams of finely cut rhizomes in 100 mL of Milli Q water were radiated in a microwave for 10 min. The aqueous extract of rhizome was cooled and filtered with Whatman No.1 filter paper and the filtrate was stored at 4 °C for further experiments.

2.3 Biosynthesis of AuNPs

The gold nanoparticles were synthesized by mixing of 1 mL of aqueous rhizome extract of *M. cochinchinensis* with 20 mL of 0.01 mM chloroauric acid ($\text{HAuCl}_4 \cdot 3\text{H}_2\text{O}$) at room temperature and the reduction of gold ions to gold nanoparticles was completed within 24 hours. The formation of gold nanoparticles was indicated by an initial visual color change from pale yellow to violet and then to ruby red color. The formation of gold nanoparticles was constantly monitored by visual inspection as well as by measuring with UV-visible absorption band in the range of 535 nm, confirming the formation of AuNPs. The AuNPs formed were found to be stable for one month.

2.4 Characterisation

The absorption spectral measurements were made using Perkin Elmer Lambda 35 (UV-Vis) spectrophotometer in the wavelength range 200–800 nm with a spectral resolution of ± 1.0 nm. The specimen was prepared by adding an AuNPs solution onto the car coated copper grid and dried in air naturally. The morphology and composition of the product were identified using high-resolution transmission electron microscopy (HR-TEM). Images of AuNPs were obtained from a JEOL JEM3010 operating at 200 kV (Icon Analytical Equipments, Mumbai, India). The crystalline nature of the synthesized AuNPs was characterized through X-ray diffraction studies using JEOL 8030 X-ray diffractometer employing CuK_α radiation. The FTIR spectra have been recorded using Perkin-Elmer Paragon-500 FTIR spectrophotometer in the wavenumber range 400 – 4000 cm^{-1} with a resolution of 4 cm^{-1} following KBr Pellet technique to identify the functional groups of the phytoconstituents.

2.5 In Vitro Antioxidant Activity

2.5.1 DPPH Radical Scavenging Activity

The DPPH Radical Scavenging assay was carried out based on the method of Ramadan-Hassanien [25]. In the DPPH radical scavenging method, 0.1 mM solution of DPPH in ethanol was prepared and 1 mL of this solution was mixed with 3 mL of sample solutions in water at different concentrations (10, 20, 30, 40 and 50 $\mu\text{g}/\text{mL}$). After 30 min, the absorbance was measured at 517 nm. A decrease in absorbance of DPPH solution indicated an increase in the DPPH radical scavenging activity. The percentage of inhibition was calculated by following equation.

$$\text{Percentage of Inhibition} = [(A_b - A_s) / A_b] \times 100 \quad (1)$$

Where, A_b is the absorbance of the blank, A_s is the absorbance for the test sample.

2.5.2 NO Radical Scavenging Activity

Nitric oxide scavenging activity was carried out by the method suggested by Basave gowda et al [26]. A stock solution of MCR aqueous extract containing 1 mg/mL was prepared with Millipore water and different amounts of the stock solution (10, 20, 30, 40 and 50 $\mu\text{g}/\text{mL}$) prepared were transferred to different test tubes and the volume was adjusted to 10 mL by the same solvent. Sodium nitro prusside, 0.2 mL (20 mM) in phosphate buffered saline (PBS; pH 7.4) and 1.8 mL of PBS solution were added to each one of these solutions and incubated at 37 °C for 3 h.

One millilitre of each solution was taken and diluted with 1 mL of Griess reagent (1% sulfanilamide, 2% phosphoric acid (H_3PO_4), 0.1% N-1-naphthyl ethylene diamine); similarly, a blank was prepared containing the equivalent amount of reagents but without the AuNPs. The absorbance of these solutions was measured at 540 nm against the corresponding blank solutions. Ascorbic acid was used as a positive control in this experiment. The percentage of inhibition was calculated by using Eq. (1).

2.5.3 Reducing Power Assay

Reducing power assay was conducted based on the method of Pulido et al [27]. Different concentrations of the aqueous plant extract in 1 mL of distilled water were mixed with phosphate buffer (2.5 mL, 0.2 M, pH 6.6) and potassium ferricyanide (2.5 mL, 1%). The mixture was incubated at 50 °C for 20 min. Trichloroacetic acid (10 %, 2.5 mL) was added to the mixture. A portion of the resulting mixture was mixed with ferric chloride (FeCl_3 ; 0.1 %, 0.5 mL) and the absorbance was measured at 700 nm in a UV-Vis spectrophotometer. In this method, ascorbic acid was used as the standard and the percentage of inhibition was calculated by using Eq. (1).

2.5.4 H_2O_2 Scavenging Activity

The H_2O_2 scavenging power was determined by following the method explained by Sroka and Cisowski [28]. A solution of H_2O_2 (40 mM) was prepared in phosphate buffer (pH 7.4). The AuNPs synthesized and the aqueous extracts of MCR at varying concentrations (10, 20, 30, 40 and 50 mg/mL) were added individually to H_2O_2 solution (0.6 mL, 40 mM). The absorbance of the reaction mixture was recorded at 230 nm. A blank containing phosphate buffer only without H_2O_2 was also performed and the percentage of inhibition was calculated by using Eq. (1).

2.5.6 Antibacterial Assay by Disk Diffusion Method

This study involves the antibacterial screening of the aqueous extract of *M. cochinchinensis* rhizomes (MCRAE) and MCR-AuNPs evaluated by disk diffusion method [29]. The microorganisms used for the experiment were standard cultures of Gram-positive bacteria *Bacillus subtilis* and *Pseudomonas aeruginosa* and gram negative bacteria *Staphylococcus aureus* and *Escherichia coli*, which were procured from the Department of Biology, GRI, Gandhigram. The microorganisms were identified by standard staining techniques and biochemical reactions. The microorganisms were maintained by sub culturing at regular time intervals on nutrient agar medium. The microorganism suspension was prepared by following the McFarland nephelometer standard. A suspension of the microorganisms containing approximately 1×10^8 cells/mL was obtained by adjusting the optical density of the suspension to that of 0.033 mL of 1.75% BaCl_2 in 10 mL of 1% H_2SO_4 . A 24 hour old culture was used to determine the zone of inhibition of the test drugs. Nutrient agar medium prepared by dissolving beef extract (3 g), peptone (5 g) and agar (15 g) in 1000 mL of distilled water was used for the preliminary anti-bacterial study to evaluate the zone of inhibition. All the necessary precautions with regard to sterilization were adopted using standard methods. 30 mL of sterile molten agar medium was allowed to solidify in sterile petridishes. A suspension of required bacterial inoculums (1×10^8 CFU/mL) was inoculated using sterile cotton swabs. Five bores were made on the medium by the use of a sterile borer. 0.1 mL of the different test drugs were added to the respective bores and allowed them to diffuse by keeping the petridishes at 4 °C in refrigerator for one hour. Streptomycin sulphate (0.1 mL, 10% solution) was taken as the standard reference in all the experiments. After the diffusion, the petridishes were incubated at 37 ± 1 °C for hours, and the zone of inhibition was observed and measured using a scale. The antibacterial activity of the test drugs was carried out against gram positive bacteria and gram negative bacteria.

3. Results and Discussion

3.1 UV-Vis Spectral Analysis

The UV-Visible absorption spectroscopy is a useful technique for assaying the formation and stability of the metal nanoparticles in aqueous solutions through the surface plasmon resonance (SPR) bands. It is well known that, the SPR bands are influenced by the size, shape, morphology, composition and the local field environment around the NPs [30]. The absorption spectrum of the MCR aqueous extract has shown in Fig. 1(a) exhibits a characteristic band at 301 nm. The disappearance of the UV-Vis absorption band at 301 nm and appearance of a new band at 535 nm could be attributed to the formation of AuNPs [31]. The UV-Vis time scan of the prepared solution of AuNPs at the room temperature shown in Fig. 1(b). The synthesized AuNPs exhibit ruby red colour, due to the excitation of

surface plasmon resonance in AuNPs. The disappearance of the band at 301 nm indicated that the precursor metal ions (chloroauric acid) are reduced to small metal ions in the presence of phenolic acids, flavonoids and other antioxidants present in MCR aqueous extract, acting both as a reducing as well as a stabilizing agent to form stable MCR-AuNPs.

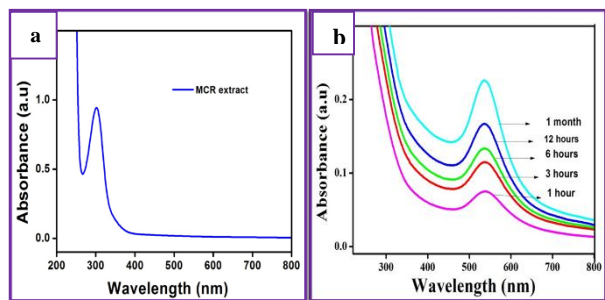


Fig. 1 UV-Vis spectrum of (a) MCR aqueous extract and (b) UV-Vis absorption spectra of MCR-AuNPs at different time intervals

Generally, the SPR bands arise due to the collective oscillations of the electrons on the surface of AuNPs (6s electrons of the conduction band for AuNPs) that is correlated with the electromagnetic field of the incoming light, i.e. the excitation of the coherent oscillation of the conductive band [32]. The reduction of Au ions and the formation of AuNPs occurred within an hour of reaction time and the SPR band in the AuNPs remains closer to 535 nm throughout the reaction time indicated that the particles are dispersed in the aqueous medium without any aggregation. Further, gradual increase in the intensity of the SPR band with increase in incubation time without any shift indicated the slow reduction of Au³⁺ to Au⁰ [33].

Furthermore, the reduction of particle size with the addition of MCR aqueous extract reveals the characteristic nature of the stabilizer/capping agent which could be useful against the aggregation and dispersion of the metal AuNPs. Moreover, the intensity of absorption band at 535 nm increases with increasing time period of aqueous component and consequent colour changes from intense yellow to ruby red colour is mainly due to the excitation of the surface plasmon resonance in the metal nanoparticles. It is concluded that, the small blue shift in SPR band width with increase in incubation time is caused by the decrease in the size of the AuNPs [34].

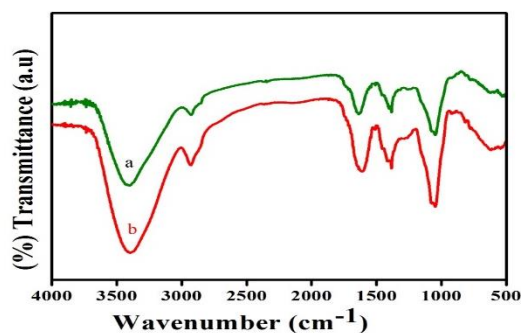


Fig. 2 IR spectrum of MCR aqueous extract and the synthesized AuNPs

3.2 FTIR Spectra

The FTIR spectra of the MCR aqueous extract and the synthesised AuNPs were recorded to identify the functional groups of the phytoconstituents present in the MCR aqueous extract that are responsible for the reduction and stabilization of the AuNPs. FTIR spectra of the MCR aqueous extract and the AuNPs (Fig. 2) exhibited several absorption bands at 3409, 2925, 1633, 1397, 1254, 1046, 910, 625, 524, 467 and 424 cm⁻¹ corresponds to various functional groups. The intense band around 3400 cm⁻¹ was attributed to hydroxyl group or amine group [35]. The bands around 1633 cm⁻¹ was corresponding to C=O stretching. The band around 1425 cm⁻¹ corresponded to C-O-H groups [36] and the absorption band at 1046 cm⁻¹ were due to the C-O stretching vibration of ether/alcoholic groups. The strong absorption bands at lower energy from 600 to 400 cm⁻¹ were mainly ascribed to the Au metal ions. It is clearly noticed from Fig. 2 that the peak positions in the wave number region 1000-400 cm⁻¹ are found to shift towards higher wave number in the FTIR spectrum of the AuNPs confirming the dual function of MCR plant extract to be possibly responsible for the reduction and stabilization of the surface of the AuNPs.

3.3 EDAX Analysis

The synthesis of MCR-AuNPs using MCR aqueous extract was further characterized by EDX analysis, which gave the additional evidence for the reduction of gold nanoparticles to elemental Au. Fig. 3 shows the EDAX spectrum of the prepared AuNPs and the adsorption peak observed around 2.30 keV indicates the presence of AuNPs due to the SPR vibration. Further, the EDAX profile for the prepared AuNPs synthesized using MCR plant extract exhibited strong peaks at 1.6, 2.30, 3.7, 8.6 0, 9.34 and 11.23 corresponding to Au atoms.

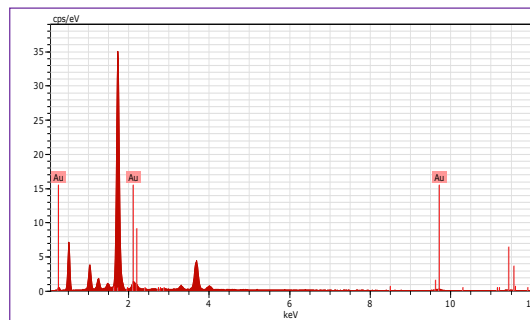


Fig. 3 EDX spectrum of MCR-AuNPs formed by MCR aqueous extract

3.4 TEM Analysis

The morphology and size of the synthesized AuNPs were investigated by HR-TEM analysis. Fig. 4 shows the HRTEM images of the prepared AuNPs for different magnification such as 100 nm (a), 50 nm (b), 10 nm (c) and 5 nm (d). It is observed from the TEM images that, the prepared AuNPs were predominantly spherical in nature and only a very few AuNPs were observed to be triangular and hexagonal in shape. It is clearly observed that all the AuNPs could be distinguished clearly from other NPs without any aggregation. Thus separation between the AuNPs was due to the presence of MCR aqueous extract acting as a capping/stabilizing agent dispersing them in the aqueous medium. The TEM images provided the size of the nanoparticles to be in the range of 16 ± 2 nm. The average size of the prepared AuNPs was calculated as 16 nm which was in good agreement with the size of the prepared AuNPs obtained in the SEM analysis.

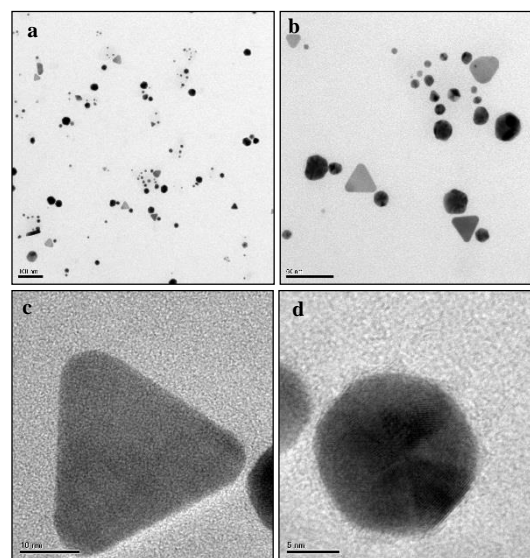


Fig. 4 TEM images of MCR-AuNPs at different magnifications: a) 100 nm, b) 50 nm, c) 10 nm and d) 5 nm

3.5 XRD Studies and SAED Pattern

The structure of the prepared AuNPs when investigated by XRD diffraction pattern revealed the formation of AuNPs having minimal surface to volume ratio. It seems from the XRD pattern that the diffraction peaks are not clearly observed which indicated that the synthesised AuNPs had spherical shape in nature and the broadening peak and noise were associated to the effect of the nanoparticles as supported by TEM and the presence of various crystalline biological molecules in the plants extracts (Fig. 5a). It is observed from the XRD pattern of AuNPs that, the

peaks at 38.19, 44.38, 64.58 and 77.57 (2θ angle) could be attributed to the crystal plane of (111), (200), (220), (311), (222), (400), (331), (420) and (422) of AuNPs which was evaluated with the JCPDS card No. 65-2870. The grain size of the prepared AuNPs was calculated from the width of the XRD peaks with the basic assumption that the nanoparticles are free from inhomogeneous strain using the Debye-Scherrer's formula $D = 0.94\lambda/\beta\cos\theta$ where D is the average crystalline domain size, λ is the X-ray wavelength (1.540 Å), β is the full width at half maximum (FWHM), and θ is the Bragg's diffraction angle of the reflecting plane and the average crystalline size of the prepared Ag-NPs was found to be 16 nm.

Fig. 4b shows the selected area electron diffraction (SAED) pattern of the prepared AuNPs and exhibited the crystalline nature and the most of the nanoparticles were spherical in shape. SAED pattern with bright circular rings corresponding to (111), (200), (220) and (311) planes exhibited the crystalline nature of the AuNPs.

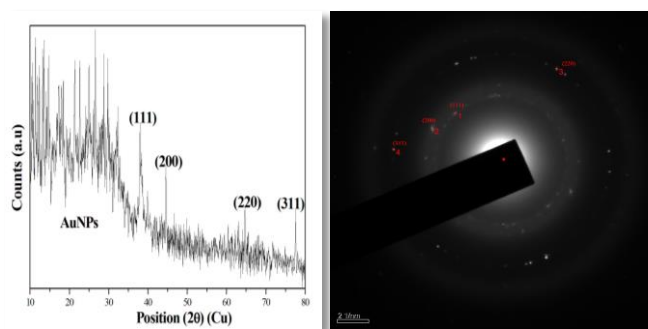


Fig. 5 a) XRD pattern of MCR-AuNPs and b) SAED pattern

3.6 Antioxidant Activity

3.6.1 DPPH Radical Scavenging Activity

The percentage of inhibition of free radical scavenging activity of the AuNPs was measured by DPPH radical scavenging assay. DPPH is a stable compound and showed a deep purple colour with a maximum absorbance at 517 nm. It will be reduced by accepting the hydrogen or electrons from antioxidant molecule coated AuNPs as well as plant extract. Percent of inhibition of DPPH radical scavenging activity of AuNPs, extract and standard ascorbic acid were presented in Table 1. Free radical scavenging activity of the AuNPs and extract on DPPH radical was found to increase with increase in concentration, showing maximum inhibition efficiency of 87.81 % and 84.14 % at 50 $\mu\text{g}/\text{mL}$ respectively. The standard ascorbic acid, however, at this concentration showed 96.48 % inhibition efficiency.

3.6.2 NO Radical Scavenging Activity

Sodium nitroprusside is known to decompose in aqueous solution at physiological pH 7.2 producing NO Under aerobic conditions, NO reacts with oxygen to produce stable products (nitrate and nitrite) and the quantities of which can be determined using Griess reagent [37]. Nitric oxide scavenging activity is used to measure the reducing tendency of MCRAE and MCR-AuNPs. NO produced when nitrite ions were reacting with superoxide molecule, which may lead to vascular system damage and results in conditions including inflammation, juvenile diabetes and multiple sclerosis. Because of the less stability of nitric oxide ions, they accept electrons from gold nanoparticles and form formazan when treated with Griess reagent that can be detected spectrophotometrically. NO Radical quenching activity of MCRAE and MCR-AuNPs increased in a dose dependent manner as seen in DPPH method [38].

3.6.3 Ferric Reducing Assay

In the reducing power assay, antioxidants forms a colored complex with potassium ferricyanide, trichloro acetic acid and ferric chloride, which is measured at 700 nm. The presence of antioxidants in samples would result in the reduction of Fe^{III} to Fe^{II} and the amount of Fe complex was monitored by measuring the formation of blue color at 700 nm. The increased absorbance at 700 nm indicated an increase in reductive ability of synthesized MCR-AuNPs. The reducing ability of the MCR aqueous extract, MCR-AuNPs and the standard drug are shown in Table 1. The results of the inhibition efficiency of test drug in concentrations of 10, 20, 30, 40 and 50 $\mu\text{g}/\text{mL}$ were monitored, MCR-AuNPs showed 82.07% while MCRAE showed 69.11% at 50 $\mu\text{g}/\text{mL}$ concentration. It is evident that the reducing powers of the MCRAE aqueous extract, MCR-AuNPs and the standard drug increased with increasing concentrations.

3.6.4 H_2O_2 Scavenging Activity

Hydroxyl radical could be produced by reaction with H_2O_2 in the presence of metal ions. (Fenton reaction) and H_2O_2 inhibition activity assay is an important method for the determination of antioxidant activity [39]. The percentage inhibition of H_2O_2 by MCRE and MCR-AuNPs are presented in Table 1. The AuNPs showed an inhibition efficiency of 77.88 % at 50 $\mu\text{g}/\text{mL}$ while that for MCRE is 65.51 % at 50 $\mu\text{g}/\text{mL}$. MCR-AuNPs showed higher anti-oxidant activity than the MCRAE in this method which may be due attachment of more antioxidant moieties at the gold ion.

Table 1 In vitro antioxidant activity of MCR extract, MCR-AuNPs using DPPH, NO, H_2O_2 and reducing power method

S. No.	Test drug	Concentration $\mu\text{g}/\text{mL}$	% of inhibition			
			DPPH method	NO method	Reducing Power assay	H_2O_2 method
1	AuNPs	10	84.06	70.72	78.92	73.18
		20	84.98	71.80	79.09	74.55
		30	85.41	72.14	80.25	75.08
		40	86.70	73.37	81.05	76.76
		50	87.81	74.53	82.07	77.58
2	MCRE	10	81.08	66.46	65.76	60.76
		20	82.93	67.22	66.34	62.09
		30	83.58	68.63	67.63	63.22
		40	83.94	70.27	68.01	64.83
		50	84.14	71.91	69.11	65.61
3	Ascorbic acid	10	92.15	80.94	88.51	81.73
		20	93.37	81.16	89.59	82.21
		30	94.68	82.96	90.11	83.00
		40	95.88	83.96	91.81	84.10
		50	96.48	84.48	92.25	85.29

3.7 Antibacterial Activity

The bacterial activity assay of MCRAE and MCR mediated AuNPs was performed at different concentrations (100, 200 and 300 $\mu\text{g}/\text{mL}$) against two selected gram negative bacteria *Escherichia coli* and *Bacillus subtilis* and two gram positive bacteria, *Pseudomonas aeruginosa* and *Staphylococcus aureus*. Among the four pathogens tested, the effect of antibacterial activity was more prominent in the case of *P. aeruginosa* (24 mm) while *E. coli* (22 mm) showed only moderate activity for *Staphylococcus aureus* (19 mm) at 300 $\mu\text{g}/\text{mL}$ of AuNPs are shown in Table 2. This may be held through the electrostatic attraction of positive charged AuNPs and negative charged cell surface of the microorganism [40]. A represents zone of inhibition of gold nanoparticles, B indicates zone of inhibition of Extract and 'C' indicates zone of inhibition of the standard antibiotic (streptomycin) respectively (Fig. 6). Comparison of the results showed that MCR-AuNPs have produced higher zone of inhibition than MCRE because of their larger specific surface area, smaller size, high penetrating power and almost spherical shape of the nanoparticles and hence facilitating the synthesized AuNPs to function as a good antibacterial agent that can be useful in biomedical applications. Recent reports suggest mechanism where gold nanoparticles functionalized with small molecules have shown good antibacterial activity [41].

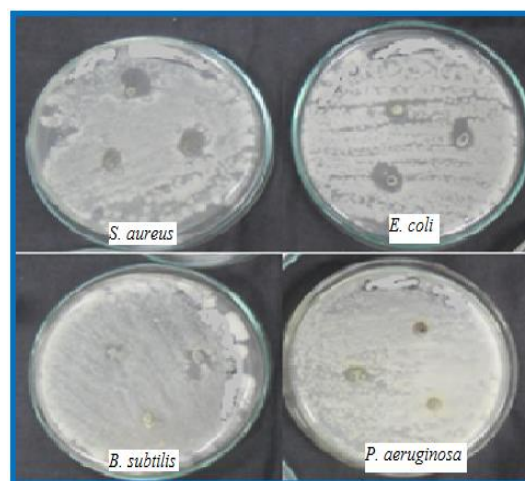


Fig. 6 Antibacterial assay of a) AuNPs, b) MCR- aqueous extract and c) standard using disk diffusion method against *S. aureus*, *B. subtilis*, *E. coli* and *P. aeruginosa*

Table 2 Antibacterial activity of MCR extract, MCR-AuNPs by Disk diffusion method

S. No.	Test drug	Concentration (µg/mL)	Zone of inhibition (mm)			
			<i>S. aureus</i>	<i>E. coli</i>	<i>B. subtilis</i>	<i>P. aeruginosa</i>
1	MCR Extract	100	05	-	08	09
		200	-	09	11	-
		300	15	18	14	11
2	MCR-AuNPs	100	08	-	-	-
		200	15	18	-	-
		300	19	22	19	24
3	Streptomycin (std)	100	25	24	30	28

4. Conclusion

Phytemediated synthesis of AuNPs has been successfully carried out using aqueous extract of the *Momordica cochinchinensis* rhizomes, acting both as a reducing as well as a stabilizing agent. Increase in reaction time increases the intensity of SPR band shifting it to blue, indicating the formation of smaller sized particles. The AuNPs synthesized were found to be a mixture of gold nanotriangular, nanorod, nano hexagonal and nonsphericals, but predominantly nonspherical. The synthesized AuNPs exhibit good anti-oxidant activity by DPPH, NO, Ferric, H₂O₂ assay methods and moderate antibacterial activity against the tested gram positive and negative pathogens.

Acknowledgment

One of the authors (A. Lakshmanan) thanks the UGC for the award of Research Fellowship for Meritorious Students to carry out this work and also the SAP to the department of Chemistry, GRI, for the facilities provided.

References

- [1] M. Mukhopadhyay, P. Dauthal, Prunus domestica fruit extract mediated synthesis of gold nanoparticles and its catalytic activity for 4 - nitrophenol reduction, Ind. Eng. Chem. Res. 51 (2012) 13014-13020.
- [2] P.J. Babu, S. Saranya, P. Sharma, R. Tamuli, U. Bora, Gold nanoparticles: sonocatalytic synthesis using ethanolic extract of Andrographis paniculata and functionalization with polycaprolactone-gelatin composites, Front. Mater. Sci. 6 (2012) 236-249
- [3] S.S. Dash, B.G. Bag, Synthesis of gold nanoparticles using renewable Punica granatum juice and study of its catalytic activity, Appl. Nanosci. 4 (2012) 55-59.
- [4] S. Krishnendu, S. Sarit Agasti, C. Kim, X. Li, M.V.M. Rotello, Gold nanoparticles in chemical and biological sensing, Chem. Rev. 112 (2012) 2739-2779.
- [5] A.K. Mittal, J. Bhaumik, S. Kumar, U.C. Banerjee, Biosynthesis of silver nanoparticles: Elucidation of prospective mechanism and therapeutic potential, J. Colloid Interface Sci. 41 (2014) 39-47.
- [6] S.S. Shankar, A. Rai, A. Ahmad, M. Sastry, Rapid synthesis of Au, Ag, and bimetallic Au core-Ag shell nanoparticles using Neem (*Azadirachta indica*) leaf broth, J. Colloid Interface Sci. 275 (2004) 496-502.
- [7] C. Sreelakshmi, N. Goel, K.K.R. Datta, A. Addlagatta, R. Ummanni, B.V.S. Reddy, green synthesis of curcumin capped gold nanoparticles and evaluation of their cytotoxicity, Nanosci. Nanotechnol. Lett. 5 (2013)1-5.
- [8] X. Jiang, D. Sun, G. Zhang, N. He, H. Liu, J. Huang, Investigation of active biomolecules involved in the nucleation and growth of gold nanoparticles by *Artocarpus heterophyllus* Lam leaf extract, J. Nanoparticle Res. 15 (2013) 1741.
- [9] M. Sastry, A. Ahmad, M. Islam Khan, R. Kumar, Biosynthesis of metal nanoparticles using fungi and actinomycete, Curr. Sci. 85 (2003) 162-170.
- [10] N. Asmathunisha, K. Kathiresan, A review on biosynthesis of nanoparticles by marine organisms, Colloids Surf. B: Biointerfaces 103 (2013) 283-287.
- [11] S. Kunjappan, R. Chowdhury, C. Bhattacharjee, A green chemistry approach for the synthesis and characterization of bioactive gold nanoparticles using *Azolla microphylla* methanol extract, Front. Mater. Sci. 8 (2014) 123-135.
- [12] O.V. Kharisova, H.V.R. Dias, B.I. Kharisov, B.O. Pérez, V.M.J. Perez, The greener synthesis of nanoparticles, Trends. Biotechnol. 31 (2013) 240-248.
- [13] B. Kaur, M. Markan, green synthesis of gold nanoparticles from *Syzygium aromaticum* extract and its use in enhancing the response of a colorimetric urea biosensor, Biosensor Bionanosci. 2 (2012) 251-258.

- [14] N. Muniyappan, N.S. Nagarajan, Green synthesis of gold nanoparticles using *Curcuma pseudomontana* essential oil its biological activity and cytotoxicity against Human ductal breast carcinoma cells T47D, J. Environ. Chem. Eng. 2 (2014) 2037-2044.
- [15] S.P. Chandran, M. Chaudhary, R. Pasricha, A. Ahmad, M. Sastry. Synthesis of gold nanotriangles and silver nanoparticles using *Aloe vera* plant extract, Biotechnol. Prog. 22 (2006) 577-583.
- [16] M.S. Akhtar, J. Panwar, Y.S. Yun, Biogenic synthesis of metallic nanoparticles by plant extracts, ACS Sustain. Chem. Eng. 1 (2013) 591-602.
- [17] D. Raghunandan, B. Ravishankar, G. Sharanbasava, D.B. Mahesh, V. Harsoor, M.S. Yalagatti, Anti-cancer studies of noble metal nanoparticles synthesized using different plant extracts, Nanotechnol. 2 (2011) 57-65.
- [18] P. Karihtala, Y. Soini, Reactive oxygen species and antioxidant mechanisms in human tissues and their relation to malignancies, Apmis. 115 (2007) 81-103.
- [19] L. Inbathamizh, T.M. Ponnuru, E.J. Mary, *In vitro* evaluation of antioxidant and anticancer potential of *Morinda pubescens* synthesized silver nanoparticles, J. Pharm. Res. 6 (2013) 32-38.
- [20] P. Dauthal, M. Mukhopadhyay, In-vitro free radical scavenging activity of biosynthesized gold and silver nanoparticles using *Prunus armeniaca* (apricot) fruit extract, J. Nanoparticle Res. 15 (2012) 1366-1367.
- [21] C. Dipankar, S. Murugan. The green synthesis, characterization and evaluation of the biological activities of silver nanoparticles synthesized from *Iresine herbstii* leaf aqueous extracts, Colloids Surf. B. Biointerfaces 98 (2012) 112-119.
- [22] S. Lokina, V. Narayanan, Antimicrobial and anticancer activity of gold nanoparticles synthesized from grapes fruit extract, Chem. Sci. Trans. 2 (2013) 105-110.
- [23] B. Edhaya Naveena, S. Prakash, Biological synthesis of gold nanoparticles using marine algae *Gracilaria corticata* and its application, Asian J. Pharm. Clin. Res. 6 (2013) 4-7.
- [24] J. Kubola, S. Siriamornun, Phytochemicals and antioxidant activity of different fruit fractions (peel, pulp, aril and seed) of Thai gac (*Momordica cochinchinensis* Spreng), Food Chem. 127 (2011) 1138-1145.
- [25] M.F.R. Hassanien, Y. Grasas, Total antioxidant potential of juices, beverages and hot drinks consumed in Egypt screened by DPPH *in vitro* assay, Aceites. 59 (2008) 254-259.
- [26] N. Basavegowda, A. Idhayadhulla, Y.R. Lee. Phyto-synthesis of gold nanoparticles using fruit extract of *Hovenia dulcis* and their biological activities, Ind. Crops. Prod. 52 (2014) 745-751.
- [27] R. Pulido, L. Bravo, F. Saura-Calixto, Antioxidant activity of dietary polyphenols as determined by a modified ferric reducing/antioxidant power assay, J. Agric. Food Chem. 48 (2000) 3396-3402.
- [28] Z. Sroka, W. Cisowski, Hydrogen peroxide scavenging, antioxidant and anti-radical activity of some phenolic acids, Food Chem. Toxicol. 41 (2003) 753-758.
- [29] Z.E. Nazari, M. Banoee, A.A. Sepahi, F. Rafii, A.R. Shahverdi, The combination effects of trivalent gold ions and gold nanoparticles with different antibiotics against resistant *Pseudomonas aeruginosa*, Gold. Bull. 45 (2012) 53-59.
- [30] S. Aswathy, D.A. Philip, Facile one-pot synthesis of gold nanoparticles using tannic acid and its application in catalysis, Phys. E. Low-Dimensional Syst. Nanostruct. 44 (2012) 1692-1696.
- [31] T.N.J.I. Edison, M.G. Sethuraman, Y.R. Lee, NaBH₄ reduction of ortho and para-nitroaniline catalyzed by silver nanoparticles using *Tamarindica indica* seed extract, Res. Chem. Intermed. (2015) 1-12.
- [32] M.C. Daniel, D. Astruc, Gold nanoparticles: assembly, supramolecular chemistry, quantum-size-related properties, and applications toward biology, catalysis, and nanotechnology, Chem. Rev. 104 (2004) 293-346.
- [33] R.K. Das, P. Sharma, P. Nahar, Synthesis of gold nanoparticles using aqueous extract of *Calotropis procera* latex, Mater. Lett. 65 (2011) 610-613.
- [34] M.R. Bindhu, M. Umadevi, Antibacterial activities of green synthesized gold nanoparticles, Mater. Lett. 120 (2014) 122-125.
- [35] S. Gurunathan, Rapid biological synthesis of silver nanoparticles and their enhanced antibacterial effects against *Escherichia fergusonii* and *Streptococcus mutans*, Arab. J. Chem. (2014) Article in Press.
- [36] D.S. Sheny, J. Mathew, D. Philip, Phytosynthesis of Au, Ag and Au-Ag bimetallic nanoparticles using aqueous extract and dried leaf of *Anacardium occidentale*, Spectrochim. Acta A: Mol. Biomol. Spectrosc. 79 (2011) 254-262.
- [37] I. Marccoci, J.J. Marguire, M.T. Droy-lefaiz, L. Packer, Review on *in vivo* and *in vitro* methods evaluation of antioxidant activity, Biochem. Biophys. Res. Commun. 201 (1994) 143-152.
- [38] N.J. Reddy, D. Nagoor Vali, M. Rani, S.S. Rani, Evaluation of antioxidant, antibacterial and cytotoxic effects of green synthesized silver nanoparticles by *Piper longum* fruit, Mater. Sci. Eng. C. Mater. Biol. Appl. 34 (2014) 115-122.
- [39] A. Serteser, M. Kargiöglu, V. Gök, Y. Bagci, M. Musa Özcan, D. Arslan, Antioxidant properties of some plants growing wild in turkey, Gracias Y. Aceities. 60 (2009) 147-154.
- [40] M.R. Bindhu, P.V. Rekha, T. Umamaheswari, M. Umadevi, Antibacterial activities of *Hibiscus cannabinus* stem-assisted silver and gold nanoparticles, Mater. Lett. 131 (2014) 10-13.
- [41] R. Gannamani, A. Perumal, S.B. Krishna, A. Mishra, K. Serphen, P. Muthusamy, N. Govender, Synthesis and antibacterial activity of silver and gold nanoparticles produced using aqueous seed extract of *protorhus longifolia* as a reducing agent, Dig. J. Nanomater. Bios. 9 (2014) 1669-1679.